The curve kick of a football I: impact with the foot

T. Asai[1], M. J. Carré[2], T. Akatsuka[3] and S. J. Haake[2]

[1]Faculty of Education, Yamagata University, Yamagata, Japan
[2]Department of Mechanical Engineering, University of Sheffield, Mappin Street, Sheffield, UK
[3]Department of Engineering, Yamagata University, Yamagata, Japan

Abstract

The purpose of this study is to assess the fundamental characteristics which cause a football to spin in a curve ball kick. The ball impact process was analysed initially with a high speed video camera running at 4500 frames per second to obtain the basic data for a computer simulation model. This simulation model showed suitable agreement although it slightly deteriorated during the latter half of impact. It was noted that rotation of the ball occurs, even if the kinetic coefficient of friction is nearly equal to 0 because of local deformation of the ball during impact around the foot allowing forces to be transmitted to the ball around its axis. The spin of the ball was found to increase with the offset distance between the foot and the axis of the ball and as the kinetic coefficient of friction was increased. The offset distance between the foot and the axis of the ball affects the spin more than the coefficient of friction. Varying the coefficient of friction from 0.0 to 1.0 produces an increase in spin of 13 rad s^{-1} at most. It was suggested that the most suitable offset distance, which makes the largest ball rotation was around 100 mm. A trade-off was found between the ball speed and spin, for different offset distances.

Keywords: biomechanics, curve kick, finite element analysis, football, soccer

Introduction

Previous studies of ball kick technique have focused on the kicking leg (Hewlett & Bennet 1951; Plagenhoef 1971; Leeds 1996). Huang *et al.* (1982) and Cabri *et al.* (1988) analysed the relationship between the motion of the kicking leg, the muscular strength and the segmental mass of the muscle. Isokawa & Leeds (1988) studied the position of the supporting leg and the angle of approach. Fabian & Whittaker (1950) pointed out the importance of the support leg position. Togari *et al.* (1982) reported that there was a close correlation between the foot joint speed and the ball speed before impact. Roberts & Metcalfe (1968) and Cooper & Glassow (1976) reported that the motion of the thigh was important to improve the leg swing speed of the kicking leg. Also, Levanon & Dapena (1998), and Anderson & Sidaway (1994) pointed out the importance of the pelvis motion. Shibukawa (1973) used the rigid body segment model of three joints for a kicking leg to simulate the momentum at impact, and pointed out that the fixation of each joint at impact was important to obtain a high ball speed. Asami & Nolte (1983) analysed the relationship between the degree of plantar flexion and the ball speed at impact, and reported the importance

Correspondence address:
Takesh Asai,
Faculty of Education,
Yamagata University Koshirakawa,
Yamagata-city, Yamagata 990-8560,
Japan.
E-mail: asai@kescriv.kj.yamagata-u.ac.jp

of providing impact on the metatarsal (toes) and the surrounding area. The kinetic studies on the kicking leg, and joint torques, has been analysed by Roberts *et al.* (1974), Zernicke & Roberts (1978), Asai *et al.* (1984) and Luhtanen (1988).

Although most of these studies have been concerned with instep kicks, in recent years the technique of curve kicks to spin the ball and bend the trajectory is becoming frequently used. Although there have been some reports about the curve ball in baseball (Briggs 1959; Mehta 1985; Watts & Bahill 1990), there are few studies about the curve kick in football (Wang & Griffin 1997; Asai *et al.* 1998).

These studies pointed out that the motion of the leg in the curve kick is more complex than that in the instep kick and that the mechanism of impact that develops the ball rotation during the impact process has not yet been determined. This study, therefore, examines the curve ball kick in football using experiment and Finite Element Analysis and focuses on the generation of spin.

Methods

Experiment

The impact process of ball kicking was analysed to obtain fundamental data for computer simulation using a high speed video camera running at 4500 frames per second. Six university football players were chosen as the subjects. The players kicked a ball with the instep toward a mini-football goal 4 m away. The high speed video camera was set up 1.5 m away from the impact with its line of sight perpendicular to the motion of the ball. The ball used in this experiment was an official FIFA ball with an internal pressure of 11 psi. The camera used was a FASTCAM-ultima (Photron Inc.) , with an image size of 256×256 pixels. Nine markers for digitizing were attached to the kicking leg of the subjects (Fig. 1). The coordinate values were digitized onto a computer using a video-position analyser. The velocities of each digitized point were calculated after digital filtering (five-point moving average) while the contact time of the foot and ball at impact was obtained by counting frames.

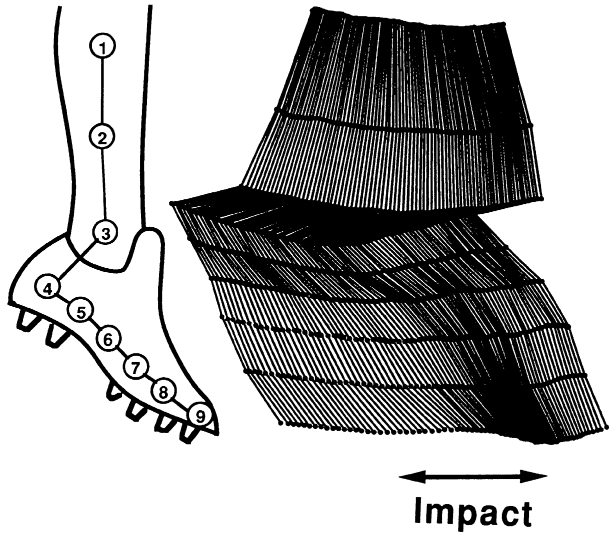

Figure 1 An example of the stick picture of the ankle joint at ball impact.

Computer simulation

The basic leg shape was determined by Asai *et al.* (1998) and constructed using a 3D digitizer. The 3D construction was meshed using MSC/PATRAN (MSC.Software Corporation) through an IGES file.

Models of the kicking leg and the surface of the ball were described by the Lagrangian frame of reference, and discretized by the finite element method. The air inside the ball was described with a Eulerian frame of reference and discretized by the finite volume method (Lenselink 1991). Hexahedron solid elements were used for the leg while shell elements were used for the ball. The air inside a ball was defined by the gamma law equation of state [$p = (\gamma - 1)\rho E$, where p is the pressure, γ the ideal gas ratio of specific heats, ρ the overall material density and E is the specific internal energy]. The number of elements for the kicking leg model in the digitized 3D curve kick model was 160 and for the drive kick model was 108. The geometry for the foot and ball models can be seen in Fig. 2.

The foot joint of the human body has a very complex structure, which consists of bones, muscles, ligaments and so on. In this study, however, a simplified model was used which assumed that the

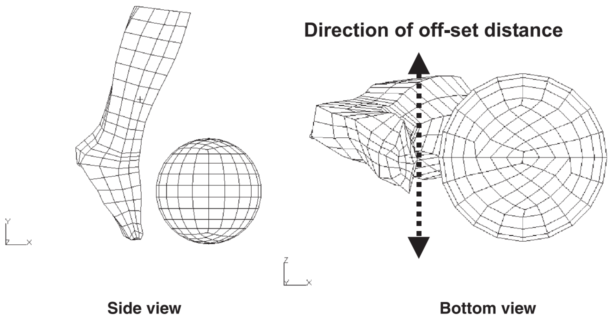

Figure 2 Foot and ball simulation models.

lower leg and foot are represented by two kinds of material properties for the calf and the foot. In both models, the Young's modulus for the foot was 30 MPa (Asai *et al.* 1996), the Young's modulus of calf was 300 MPa and the Poisson's ratio was 0.3 (Beaugonin & Haug 1996).

The total mass used in both the curve kick model and drive kick model was 4.0 kg. As an initial condition of impact, the angular velocity was set such that the velocity on the impact part of the foot was 25 m s^{-1} about an axis located in the top end node.

During the analysis of an impact force, the initial speed in the horizontal direction (25 m s^{-1}) was assumed for the entire part of the kicking leg in both models.

The generation of spin depends upon the location of the impact point of the foot on the ball in relation to the axis of the ball. This impact distance was set at 40 and 80 mm from the ball's axis and simulation was carried out for coefficient of friction values between 0 and 1.0 at intervals of 0.2. Further simulations were carried out with a fixed coefficient of friction of 0.4 with impact distances from the axis of the ball −150 to +150 mm at intervals of 20 mm.

The pressure distributions and impact forces at impact for both cases using the digitized 3D instep kick model and digitized 3D infront kick model were compared with each other. In this study, the impact force was solved using equations (1) and (2).

$$F = \frac{FACT \times W_{\mathrm{mass}}}{(\Delta t)^2} \delta \cdot \bar{n} \quad (1)$$

$$W_{\mathrm{mass}} = \frac{M_{\mathrm{t}} \times M_{\mathrm{s}}}{M_{\mathrm{t}} + M_{\mathrm{s}}} \quad (2)$$

where δ is the node distance of penetration, F the contact force, M_{t} the mass of the master segment, M_{s} the mass of the slave segment, δt the time step, $FACT$ the scale factor and $\bar{n}$ is the normal vector.

In this study, MSC/DYTRAN, an explicit integral solver, was used as the solver in each simulation. MSC/PATRAN was used for pre- and post-data processing.

Results and discussion

Experiment

A stick picture of the ankle joint during a typical ball impact for a curve kick is shown in Fig. 1. The stick picture covers a duration of approximately 20 ms while the impact lasts approximately 9 ms. It can be seen that points 7, 8 and 9 (i.e. the toes and end portion of the foot) are clearly retarded during impact while the higher part of the ankle and leg continues almost at the same speed. This indicates significant deformation of the foot during impact, which could not be accounted for in a rigid body model.

The horizontal velocity of points on the foot during a typical impact is shown in Fig. 3. Point 3 is almost on the ankle (the lateral malleolus of the ankle joint) while point 8 is near the end of the foot

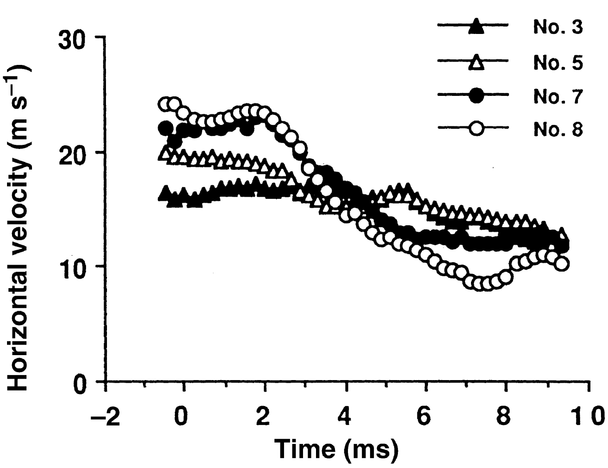

Figure 3 The horizontal velocity of each measurement point of the ankle joint during the impact.

Table 1 The ball velocity, impulse, contact time, contact distance and foot velocity in experiment

	Sub.	A	B	C	D	E	F	Mean	SD
Ball velocity	(m/s)	25.17	25.21	24.46	25.96	26.98	25.21	25.44	0.76
Impulse	(Ns)	10.93	10.96	10.63	11.28	11.59	10.96	11.06	0.33
Contact time	(ms)	9.33	9.33	8.88	9.11	8.67	9.33	9.12	0.28
Contact distance	(m)	0.144	0.158	0.143	0.150	0.137	0.150	0.147	7.28
Foot (no.7) velocity	(m/s)	23.83	22.17	21.92	22.90	24.66	23.22	23.12	1.03

(the fifth metatarsal bone). It can be seen that the change in velocity during impact was higher at the end of the foot than at the ankle indicating greater decelerations, forces and deformations.

The data for the six subjects studied is shown in Table 1. The mean value of ball speed for the subjects was 25.44 m s^{-1} while the mean contact time was 9.12 ms. Zernicke & Robert (1978) found velocities of 27.4 m s^{-1} in a similar study while Asami & Nolte (1983) found contact times of 12 ms. The differences between the current results and previous data can be accounted for by differences in leg swing speed and biomechanical differences in the players. The foot velocity data was based on the velocity of point 7 (shown in Fig. 1).

Table 1 shows that the foot moved, on average 147 mm while in contact with the ball, representing approximately 66% of the diameter of the ball (223 mm).

Validating the FE model

Figure 4 shows the horizontal velocity of the toe (point 8, the metatarsal) during impact for the finite-element model and the experiment. The model shows reasonable agreement with the experimental data, particularly in the first half of the impact. Figure 5 shows the simulated deformations of the foot and ball during impact at intervals of 1 ms. The ball deformed to 85% of its original diameter in the model compared to 86% experimentally. It was considered that the model matched the experimental data well enough to warrant use for further study.

Coefficient of friction and spin

Figure 6 shows the variation of spin with coefficient of friction for impacts at 40 and 80 mm from the axis of the ball. It can be seen that the spin increases as the coefficient of friction increases and that doubling the offset from the axis of the ball roughly doubles the spin. These results are expected intuitively because a high coefficient of friction stops the foot slipping across the surface of the ball and a large offset of impact point from the centre of mass allows the foot to apply a greater torque to the ball. It is interesting to note that, even at zero coefficient of friction, spin can still be imparted to the ball. This is because of local deformation of the ball during impact around the foot allowing forces to be transmitted to the ball around its axis. Clearly, the offset from the ball's axis has a much larger effect than a variation in the coefficient of friction.

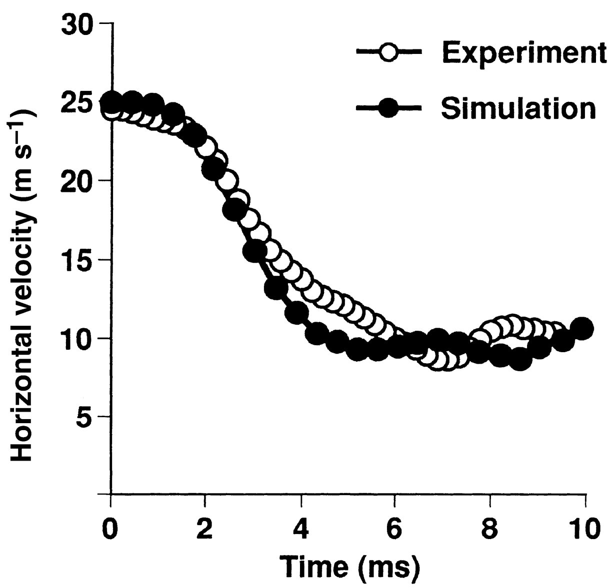

Figure 4 The horizontal velocity of the toe point at impact for both the experiment and stimulation.

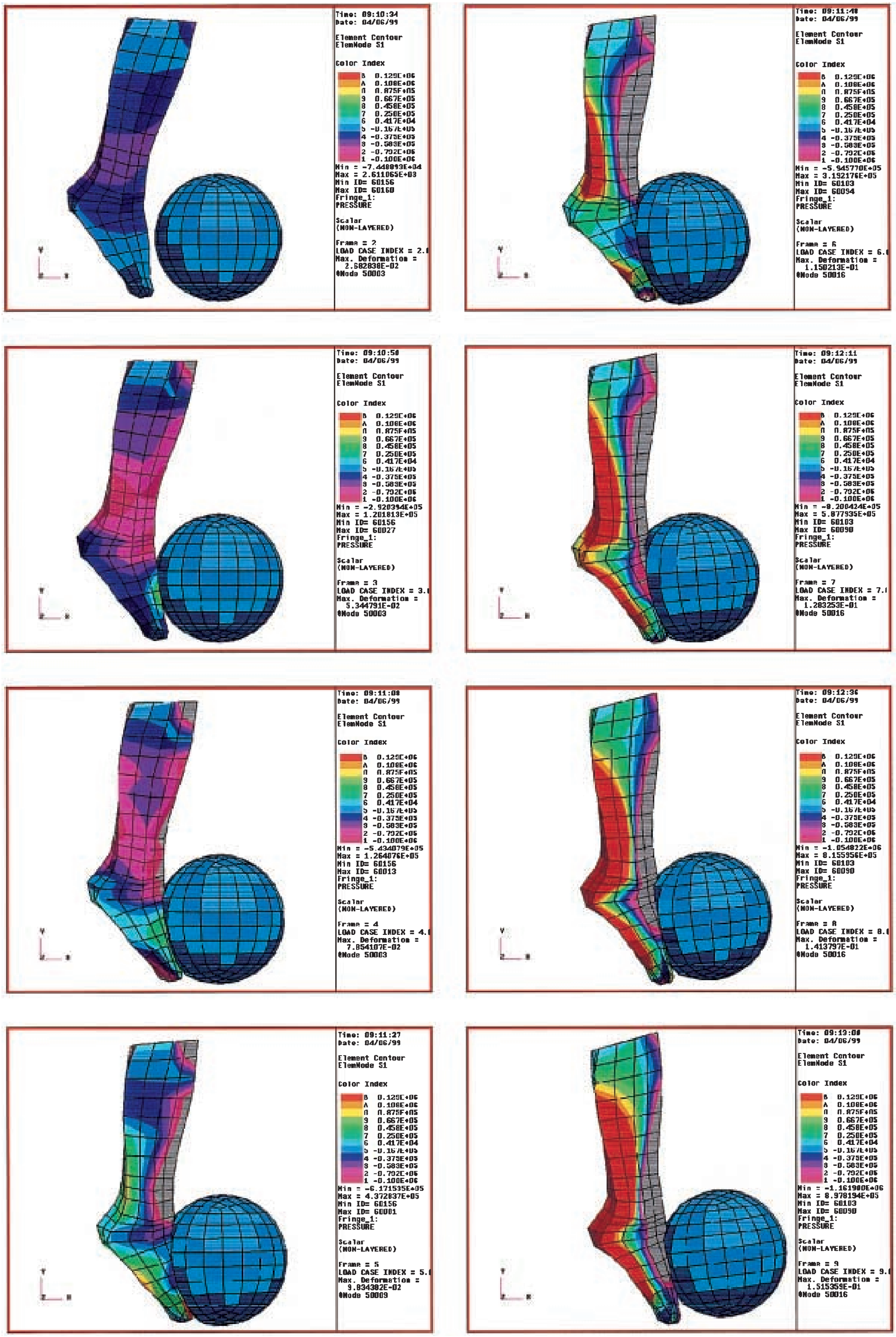

Figure 5 The pressure contours on the deformed shape during impact using the digitized 3D instep kick model.

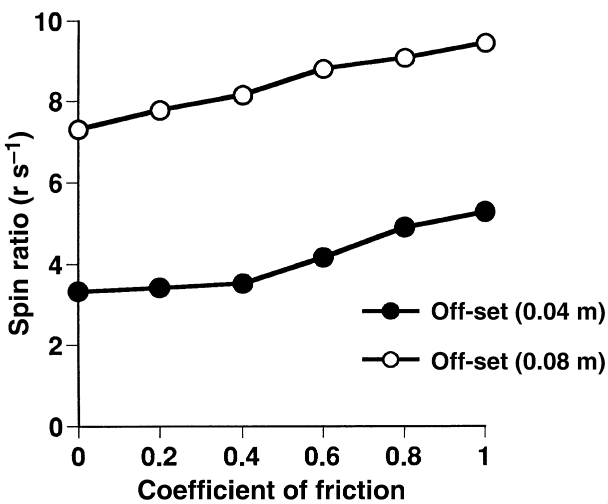

Figure 6 The relation of the spin ratio and the coefficient of friction.

Table 2 Comparison of offset distance, spin ratio and ball velocity using digitized 3D instep kick model

Case no.	Offset distance (m)	Spin ratio (r/s)	Ball velocity (m/s)
Case 7	−0.16	−10.6	6.2
Case 8	−0.14	−13.0	10.9
Case 9	−0.12	−11.0	15.2
Case 10	−0.10	−9.7	19.0
Case 11	−0.08	−8.2	20.5
Case 12	−0.06	−5.7	22.9
Case 13	−0.04	−3.5	23.5
Case 14	−0.02	−3.0	25.5
Case 15	0.0	−1.9	26.0
Case 16	0.02	0.8	25.9
Case 17	0.04	4.0	23.1
Case 18	0.06	6.9	20.7
Case 19	0.08	10.5	18.5
Case 20	0.10	14.6	15.1
Case 21	0.12	16.2	11.2
Case 22	0.14	9.7	4.5
Case 23	0.16	0.0	0.0

Effect of the offset of the impact point from the axis of the ball

Offset distance, ball spin and ball speed

The relation between the offset distance of the impact part to the centre of the ball and the spin was examined using the digitized 3D instep kick model. Simulations for 17 steps which moved the impact point in each direction of ± 0.16 m on both sides in 0.02 m increments from the centre of the ball were carried out (the coefficient of friction was fixed at 0.4) (Table 2).

Figure 7 shows that although the spin increases in accordance with an increase in the offset distance, it rapidly decreases after the offset distance exceeds the radius of the ball. The foot continues to impact with ball because it has finite width. In comparison, the ball speed decreased with an increase in the offset distance.

These results suggest that in the case when the offset distance approaches the radius of the ball, the contact area and time rapidly decrease and the energy of the impact is only slightly transferred. Hence, it is suggested that the ball rotation and the ball speed are related to a trade-off of offset distance, within the range of the radius of the ball.

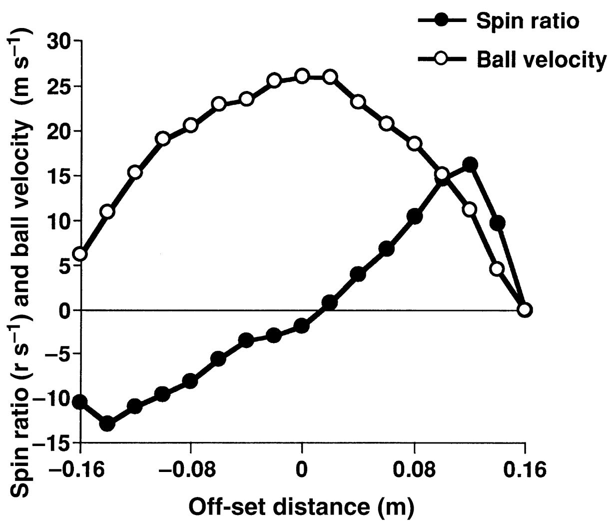

Figure 7 The relation of the offset distance, spin ratio and ball speed.

Impact force during ball kick

The simulations up to now were carried out using the digitized 3D instep kick model with the shape model extended ankle to make it easy to understand the fundamental characteristics and interactions. However, for a curve kick, not only the out front kick whose shape is similar to the shape of the instep kick, but the infront kick with an ankle bent into the shape of an 'L', is also often used. Using the digitized 3D instep kick model and the digitized 3D infront kick model, this study then analysed the pressure distribution and the impact force at impact during the instep kick and the infront kick. Also, the shape of the infront kick model was with the ankle bent rectangularly and rotated outside 45 deg, and the offset distance was 0.02 m.

The pressure contours on the deformed shape at 4 ms after the impact for the simulation result using the digitized 3D instep kick model are shown in Fig. 8.

High compressive pressure is seen not only in the impact part but in the plantar as well, and tensile pressure is observed in the shin. The maximum pressure at this time was 126 KPa, while the minimum pressure was −543 KPa.

The pressure contours on the deformed shape at 4 ms after the impact for the simulation result using the digitized 3D infront kick model are shown in Fig. 9.

High compressive pressure is seen not only in the impact part but also in the plantar as well, and tensile pressure is observed in the back of the ankle joint. The maximum pressure at this time was 345 KPa, while the minimum pressure was −436 KPa. Also, for this simulation, the rotation speed of the ball was 32.7 rad s^{-1}.

From the analysis of the stress and pressure distributions, it is postulated that the improvement in traction on the metatarsal, navicular and cuneiform against the ball will increase the spin of the ball for the infront curve kick.

The impact forces of the instep kick and the infront curve kick based on computer simulations are shown in Figs 10 and 11. The peak value of the horizontal impact force in the instep kick was 2439 N, that of the vertical impact force was 853 N, and that of the lateral impact force was −452 N. On the other hand, the peak value of the horizontal impact force for the infront curve kick was 2206 N, that for the vertical impact force was 1221 N, and that for the lateral impact force was −1143 N.

It appears that the vertical and lateral forces generate a net force which increases the rotation of the ball as well as the flight of the ball in a direction different from the swing direction of the kicking leg.

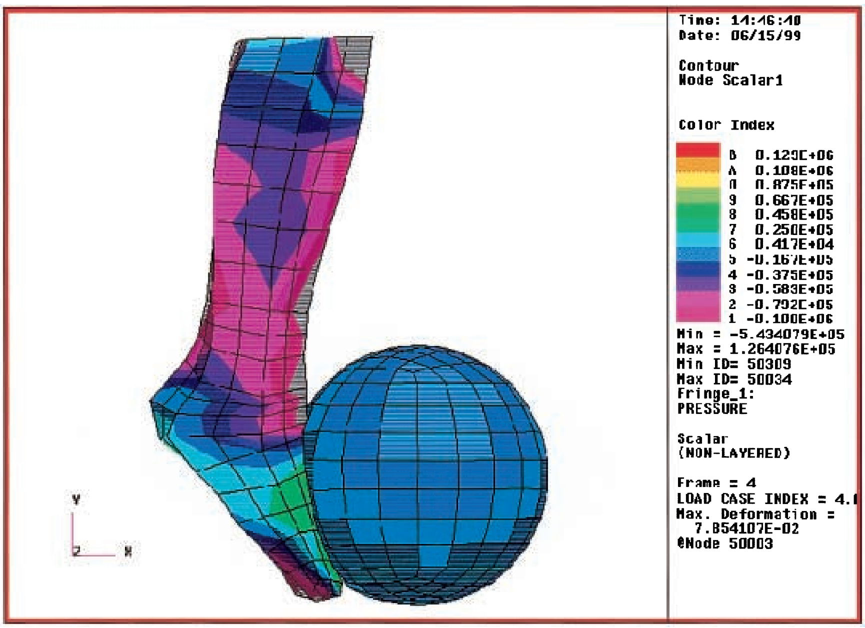

Figure 8 The pressure contours on the deformed shape at 4 ms after impact using the digitized 3D instep model.

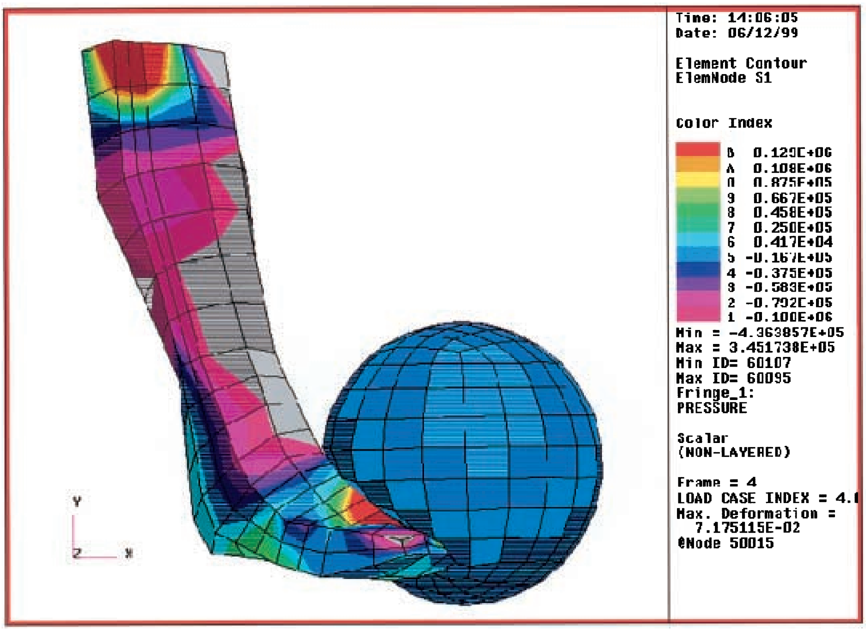

Figure 9 The pressure contours on the deformed shape at 4 ms after impact using the digitized 3D infront model.

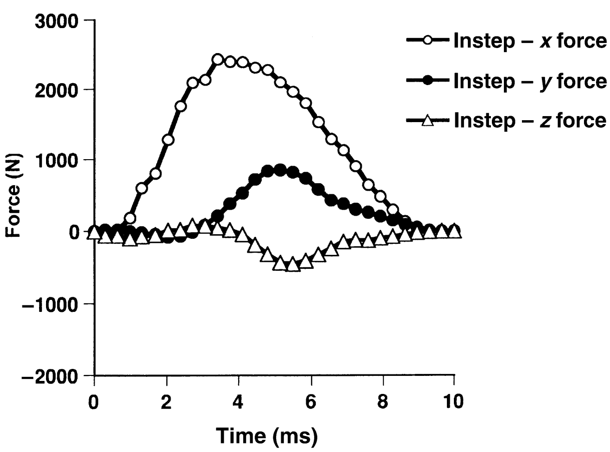

Figure 10 The impact forces of the instep kick based on computer simulation.

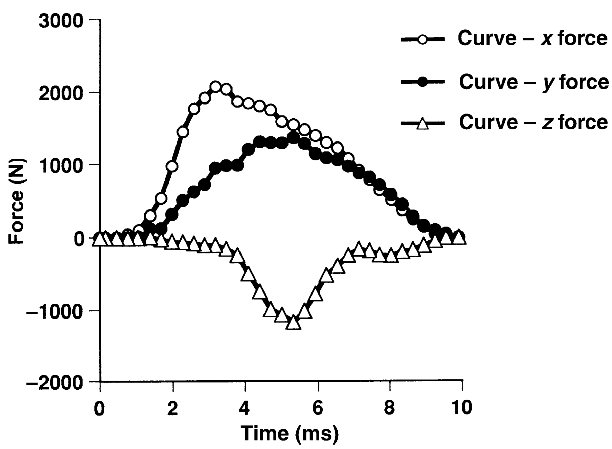

Figure 11 The impact forces of the infront curve kick based on computer simulation.

Conclusions

The first objective of this study was to clarify the fundamental characteristics which cause ball rotation using a computer simulation with Coupled Fluid-Structure Interaction Finite Element Analysis, after analysing the ball impact process by a high speed video camera (4500 fps) to obtain the input data for the model.

The experimental results from the high speed video camera showed that the mean of the contact distances was 0.147 m and the contact of the ball and instep was finished before the instep moved the same distance as the ball diameter (about 0.223 m).

From the computer simulations, it was noted that even if the kinetic coefficient of friction is even equal or nearly equal to 0, rotation of the ball occurs, although it is axiomatic that the spin of the ball increases with the increase in the kinetic coefficient of friction in both simulations. It seems that a large deformation appeared during the impact of the ball and that causes the rotation because of the impact force. Overall, it is considered that the offset distance affects ball spin more than a coefficient of friction.

It was suggested that the optimum offset distance is related to a trade-off between ball rotation and ball speed.

The peak value of the horizontal impact force in the instep kick was 2439 N, that of the vertical impact force was 853 N, and that of the lateral impact force was −452 N. On the other hand, the peak value of the horizontal impact force for the infront curve kick was 2206 N, that for the vertical impact force was 1221 N, and that for the lateral impact force was −1143 N.

It appears that the vertical and lateral forces generate a net force that increases the rotation of the ball as well as the flight of the ball in a direction different from the swing direction of the kicking leg.

The computational simulation model used in this study has a simple shape and structure, and the actual phenomena cannot be completely reproduced. It is considered that the results shown in this study provide a foundation to appreciate the essential mechanism of the phenomena, although these only clarify the fundamental characteristics and properties of some individual phenomenon. These will provide useful references when we will design a more precise analysis model and more accurate analysis method in the future.

References

Asai, T., Kobayashi, K., Morioka, R. & Matsumoto, M. (1984) A study of kicking motion in Soccer. University of Tsukuba. *Bulletin of Health and Sports Sciences* **7**, 49–54.

Asai, T., Akatsuka, T. & Kamata, Y. (1996) Impact Simulation of Kicking using Fluid and Structure Interaction Analysis. *Proc. XIV Int. Symp. Biomech. Sports*, 588-591.

Asai, T., Akatsuka, T., Nasako, M. & Murakami, O. (1998) Computer simulation of curve-ball kicking in soccer. In: *The Engineering of Sport* (ed. S.J. Haake), 433–440, Blackwell Science, Oxford, UK.

Anderson, D.I. & Sidaway, B. (1994) Coordination changes associated with practice of a soccer kick. *Res. Q. Exerc. Sport*, Washington, DC, AAHPERD, **65**, 93–99.

Asami, T. & Nolte, V. (1983) Analysis of powerful ball kicking. In: *Biomechanics VIII-B* (eds H. Matsui & K. Kobayashi), pp. 695–700, Human Kinetics Publisher, Champaign.

Beaugonin, M. & Haug E. (1996) A numerical model of the human ankle/foot under impact loading in inversion and eversion, *SAE 962428*, 239–249.

Briggs, L.J. (1959) Effect of spin and speed on the lateral deflection (curve) of a baseball; and the Magnus effect for smooth spheres. *Am. J. Phys.*, **27**, 589–596.

Cabri, J., De Proft, E., Dufour, W. & Clatys, J.P. (1988) The relation between muscle strength and kick performance. In: *Science and Football* (eds T. Reilly, A. Leeds, K. Davids & W.J. Murphy), pp. 186–193, E and FN spon Ltd, New York.

Cooper, J.M. & Glassow, R.B. (1976) *Kinesiology*. C.V. Mosby Co., St Luis, 167–170.

Fabian, A.H. & Whittaker, T. (1950) *Constructive football*. Edward Arnold and Company, London.

Hewlett, J.M. & Bennet, B.L. (1951) Fundamental Kicking in Soccer. *The Athletic Journal XXII.* (November), Vol. 32, Claredon Press, New York.

Huang, T.C., Roberts, E.M. & Youm, Y. (1982) Biomechanical of Kicking. In: *Human Body Dynamics, Impact, Occupational and Athletic Aspects* (ed D.N. Ghista), pp. 409–441, Clarendon Press, New York.

Isokawa, M. & Leeds A. (1988) A Biomechanical analysis of the instep kick motion in soccer. In: *Science and Football* (eds T. Reilly, A. Leeds, K. Davids & W.J. Murphy), pp. 449–455, E and FN spon Ltd, New York.

Leeds, A. (1996) Biomechanics applied to soccer skills. In: *Science and Soccer* (ed. T. Reilly), pp. 123–133, E and FN spon Ltd., New York.

Lenselink, H. (1991) *Oblique penetration in ductile plates.* MSC paper 91–03, The MacNeal Schwendler Corporation.

Levanon, J. & Dapena, J. (1998) *Comparison of the kinematics of the full-instep and oass kicks in soccer*. American College of Sports Medicine, Madison, WI, USA. *Med. Sci. Sports Exerc.*, **30**, 917–927.

Luhtanen, P. (1988) Kinematics and kinetics of maximal instep kicking in junior soccer players, In: *Science and Football* (eds T. Reilly, A. Leeds, K. Davids & W.J. Murphy), pp. 441–448, E and FN spon Ltd, New York.

Plagenhoef, S. (1971) *Patterns of Human Motion*, pp. 98–116. Prentice Hall, Englewood Cliffs, NJ.

Roberts, E.M. & Metcalfe, A. (1968) In: *Biomechanics I* (eds J. Wartenweiler, E. Jokl & M. Hebbelinck), pp. 315–319, University Park Press, Baltimore.

Roberts, E.M., Zernicker, R.F., Youm, Y. & Hung, T.C. (1974) Kinetic parameters of kicking. In: *Biomechanics IV* (eds R. Nelson & C. Morehouse), pp. 157–162, University Park Press, Baltimore.

Shibukawa, K. (1973) *Effect of joint fixing when kicking a soccer ball*. The faculty of physical education, Tokyo University of Education. *Bull. Inst. Sports Sci.*, **11**, 81–83.

Wang, J.S. & Griffin, M. (1997) Kinematic analysis of the soccer curve ball shot. *Strength Conditioning*, February, 54–57.

Watts R.G. and Bahill, T.A. (1990). *Keep Your Eye on the Ball: The Science and Folklore of Baseball*. W.H. Freeman and Company, New York.